Hyper-Hue and EMAP on Hyperspectral Images for Supervised Layer Decomposition of Old Master Drawings

AmirAbbas Davari[1], Nikolaos Sakaltras[1], Armin Häberle[2], Sulaiman Vesal[1], Vincent Christlein[1], Andreas Maier[1] and Christian Riess[1]

[1]Pattern Recognition Lab, Department of Computer Science, Friedrich-Alexander University Erlangen-Nürnberg, Erlangen, Germany

[2]Bibliotheca Hertziana - Max-Planck-Institute for Art History, Rome, Italy

Introduction

- Old master drawings were mostly created step by step in several layers using different materials
- Processing of these layers bring useful information about the creation evolution of the drawing
- Layers are overlaid/diluted
- Molecular spectroscopy is destructive.
- Hyperspectral image analysis can potentially separate the layers

Aim:

- Using hyperspectral (HS) images to separate these layers
- Comparing the performance of two powerful descriptors:
  (1) Hyper-hue [1]
  (2) Extended multi-attribute profiles [2]
- Introducing the spectral focus stacking

Hyper-hue [1]

- The vector connecting the n-dimensional points, Hyper-Black to Hyper-White is the achromatic hyper-axis **a**
- hyper-axis is the normal vector of the hyper-chromatic plane **c**
- Hyper-hue is a function of hyper-pixels (**x**) projections on the hyper-chromatic plane
- There are *n-1* Spanning unit vectors $\mathbf{u}_i$ of the n-dimensional hyper-chromatic plane

Hyper-hue $h = \frac{c}{\|c\|}$

Saturation $S = \mathrm{Max}\{x_1, x_2, \ldots, x_n\} - \min\{x_1, x_2, \ldots, x_n\}$

Intensity $I = (1/n)(x_1 + x_2 + \ldots + x_n)$

EMAP [2]

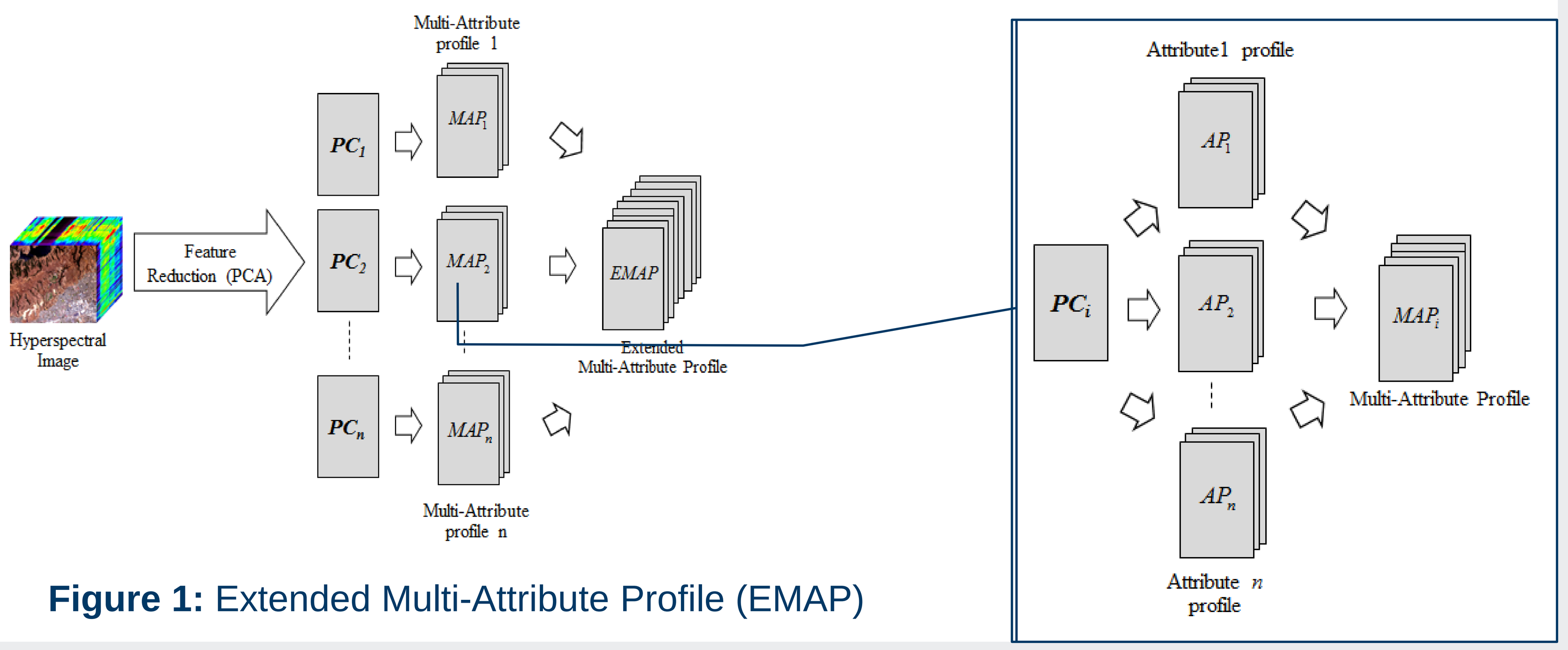

Figure 1: Extended Multi-Attribute Profile (EMAP)

Phantom Data and its Hyperspectral Image

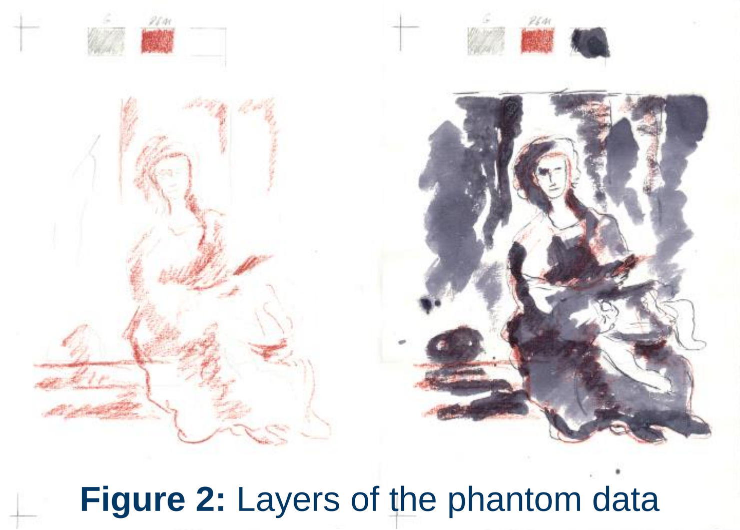

Figure 2: Layers of the phantom data

Figure 3: Raw HS image, channels 20, 40, 70, 130 and 230

Pipeline

Figure 4: Sensitivity normalization

Figure 5: Illumination correction

Figure 6: H_1 which is focused on the blue spectrum vs. H_2 which is focused on the red spectrum. (a) H_1 channel 41 (457.82 nm), (b) H_2 channel 41 (457.82 nm), (c) H_1 channel 200 (854.97 nm), (d) H_2 channel 200 (854.97 nm). Different focused channels. Solution? Spectral focus stacking.

Figure 7: Simulated RGB images from raw HS image, sensitivity normalized HS image and illumination corrected HS image.

Results

Feature	AA% (±SD)	OA% (±SD)	Kappa (±SD)
SimRGB	71.83 (±0.79)	62.05 (±1.90)	0.3632 (±0.0178)
SimRGB-IC	73.72 (±1.10)	64.96 (±2.40)	0.3980 (±0.0257)
SimRGB-IC-SI	74.29 (±0.61)	66.08 (±2.57)	0.4119 (±0.0261)
SimRGB-IC-EMAP	74.63 (±0.77)	67.25 (±1.84)	0.4251 (±0.0170)
HSI	75.43 (±1.05)	66.94 (±2.11)	0.4196 (±0.0217)
HSI-IC	76.57 (±0.94)	67.21 (±3.56)	0.4304 (±0.0366)
HSI-DR	80.35 (±0.66)	72.58 (±1.53)	0.5019 (±0.0183)
HSI-h	**83.00** (±0.47)	**77.39** (±1.28)	**0.5731** (±0.0161)
HSIhSI	82.86 (±0.52)	77.16 (±1.53)	0.5701 (±0.0213)
HSIhSI-DR	79.58 (±0.86)	71.00 (±2.41)	0.4817 (±0.0273)
HSI-EMAP	**82.61** (±1.11)	**77.35** (±2.53)	**0.5719** (±0.0350)
HSIhSI-EMAP	**83.08** (±0.89)	**77.70** (±1.18)	**0.5766** (±0.0191)

Table 1: Quantitative results using random forest classifier. It can be observed that variants of hyperspectral image result in better classification performance comparing to RGB variants. Best accuracy is obtained by combination of EMAP and hyper-hue.

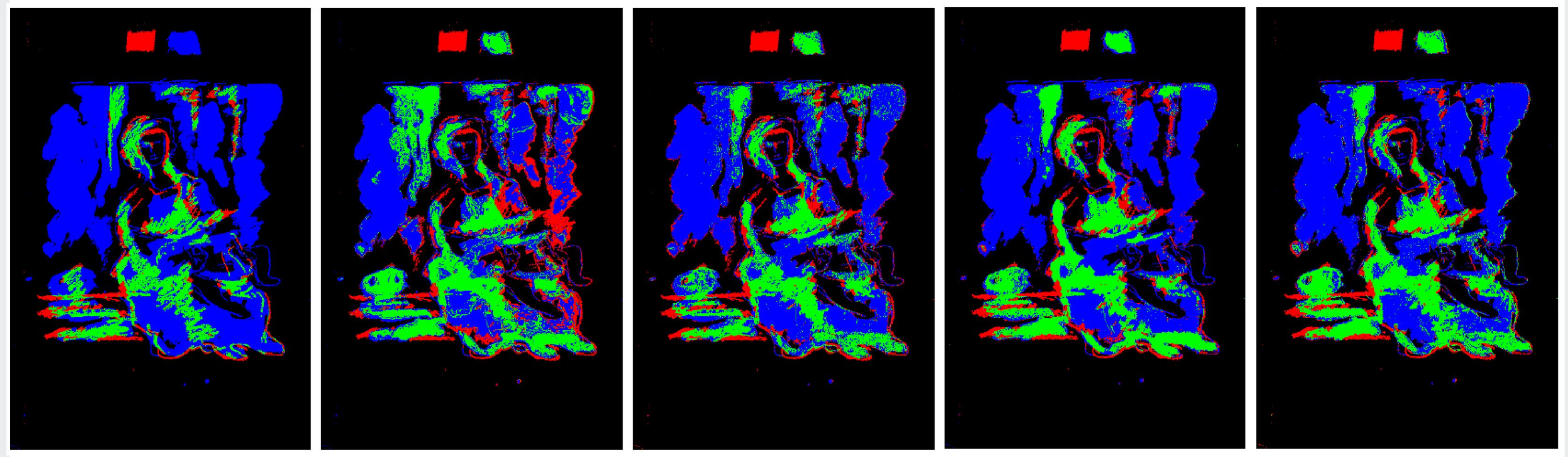

Figure 8: Qualitative results. From left: 1) ground truth, 2) Sim-RGB, 3) HSI-h, 4) HSI-EMAP, 5) HSIhSI-EMAP. Green color represents the areas with overlapping red chalk and black ink.

Conclusion

- HS images result in better layer separation compare to RGB images
- EMAP and hyper-hue, both outperform the raw HS image
- Spectral focus stacking improves the layer separation

Limitations of hyperspectral cameras, which can be addressed by using multispectral cameras:

- Low signal to noise ratio
- low resolution

References

[1] H. Liu, S.-H. Lee, and J. S. Chahl, “Transformation of a high-dimensional color space for material classification,” JOSA A, vol. 34, no. 4, pp. 523–532, 2017.

[2] M. Dalla Mura, J. A. Benediktsson, B. Waske, and L. Bruzzone, “Morphological attribute profiles for the analysis of very high resolution images,” IEEE Transactions on Geoscience and Remote Sensing, vol. 48, no. 10, pp. 3747–3762, 2010.